iJRASET
International Journal For Research in Applied Science and Engineering Technology

INTERNATIONAL JOURNAL FOR RESEARCH

IN APPLIED SCIENCE & ENGINEERING TECHNOLOGY

Volume: 7 **Issue:** VII **Month of publication:** July 2019

DOI: http://doi.org/10.22214/ijraset.2019.7030

www.ijraset.com

Call: 08813907089 | E-mail ID: ijraset@gmail.com

International Journal for Research in Applied Science & Engineering Technology (IJRASET)
ISSN: 2321-9653; IC Value: 45.98; SJ Impact Factor: 7.177
Volume 7 Issue VII, July 2019- Available at www.ijraset.com

Optimization of Hybrid Journal Bearing using Artificial Neural Network and Genetic Algorithm

K. G. Ravindra[1], Manohar H.S.[2], T. Nagaraju[3]
[1, 2, 3] *Department of Mechanical Engineering, P E S College of Engineering, Mandya 571 401,Karnataka*

Abstract: ***A rapid and globally convergent predictive tool for optimization of capillary compensated hole-entry hybrid journal bearing having transverse roughness pattern is developed using Artificial Neural Network (ANN) and Multi Objective Genetic Algorithm (MOGA). ANN is trained to compute the objective functions for the multi-objective GA optimization problem of hybrid journal bearing. Five most important parameters such as supply pressure, restrictor design parameter, dynamic viscosity of oil, surface roughness characteristics of opposing surfaces (i.e. variance ratio) and roughness pattern parameter are selected as design variables. Minimum fluid film thickness, frictional torque and critical journal mass of capillary compensated hybrid journal bearing are selected as objective functions. The optimum values of design variables are obtained by interfacing multi-objective GA with ANN. The optimization goal is to maximize the minimum oil film thickness and critical journal mass and to minimize frictional torque on journal surface as three objectives and is achieved using a Pareto optimal front. Achievement of regression value above 99% and close agreement between expected and predicted value of all the three output functions shows the suitability of ANN in Multi-objective Genetic Algorithm optimization problem.***

Keywords: Hybrid Journal Bearing, Artificial Neural Network, Genetic Algorithm, Pareto Optimal Front.

I. INTRODUCTION

A hybrid journal bearing basically combines the mechanism of hydrostatic and hydrodynamic lubrication principles to achieve load support at low as well as high speed and provides superior performance as compared to hydrostatic journal bearing. Hybrid journal bearings have been widely used to support high speed rotating machinery such as turbines, compressors and pumps. These bearings operate continuously at high speed and heavy loads.

Generally, the performance characteristics of journal bearings are governed by a number of geometric and operating parameters such as radial clearance, length to diameter ratio, supply pressure, etc. Thus, the selection of these parameters is most essential for the optimum performance of journal bearings and hence little amounts of works in the area of journal bearing optimization have been carried out and reported in the available literature. Hashimoto [1] proposed a hybrid optimization technique that combines the direct search and successive quadratic programming methods for the optimization of cylindrical journal bearing and Hashimoto and Matsumoto [2] extend this method for the optimization of elliptical journal bearing. Wang et. al [3] used the unconstrained nonlinear programming, lattice search and simplex methods for the optimization of lobe bearing. Hirani and Suh [4] developed a Pareto-optimal front for hydrodynamic journal bearing and solved its multi objective optimization using genetic algorithm. Using genetic algorithm Boedo and Eshkabilov [5] performed the optimal shape design of a finite width journal bearing. Ghorbanian et al. [6] used a neural network and multi-objective genetic algorithm models as rapid and globally convergent predictive tool for the optimization of dynamically loaded journal bearings. Kirankumar and Prajapati [7] and Roy and Kakoty [8] also utilized the Pareto optimal concepts of genetic algorithm and optimized their journal bearing systems. Genetic Algorithm in interface with Artificial Neural Network gives the optimized values of design variables from Pareto front and it provides a number of options to select the bearing parameters obtained from Pareto optimal design [9]. Hence, it was planned to use a more efficient ANN and GA to carry out optimization of journal bearing considering surface roughness effects.

An Artificial Neural Network (ANN) has been developed to compute the output for objective function such as minimum fluid film thickness, frictional torque and critical journal mass of capillary compensated hole-entry hybrid journal bearing for the selected geometric and operating parameters. Achievement of regression value above 99% and close agreement between expected and predicted value of all the three output functions shows the suitability of ANN in Multi-objective genetic algorithm optimization problem. A genetic algorithm was then applied to the trained ANN model to determine the design parameters that would result in the optimal value of the objective functions of hybrid journal bearing. Using Multi-objective Genetic Algorithm (MOGA) technique, the maximization of minimum oil film thickness and critical journal mass as well as the minimization of frictional torque has been carried out for the capillary compensated hole-entry hybrid journal bearing having transverse roughness pattern.

ISSN: 2321-9653; IC Value: 45.98; SJ Impact Factor: 7.177
Volume 7 Issue VII, July 2019- Available at www.ijraset.com

II. NOMENCALTURE

Dimensional Parameters

c = Radial clearance, μm
e = Journal eccentricity, mm
h = Nominal fluid-film thickness, mm
h_L = Local fluid-film Thickness, mm
h_T = Average fluid-film thickness, mm
R_J = Radius of journal, mm
p = Pressure, N.mm^{-2}
p_s = Supply pressure, N.mm^{-2}
x = Circumferential coordinate, mm
y = Axial coordinate, mm
z = Coordinate across fluid-film thickness, mm
ε = Eccentricity ratio, e/c
p_S =Supply Pressure, N/mm^2
Q =Lubricant flow, mm^3/sec
λ = Aspect ratio, L/D
$\lambda_{0.5x,y}$ = 0.5 correlation lengths of the x and y profile, μ m
μ = Dynamic viscosity of lubricant, Pas
σ = RMS value of combined roughness, $\sqrt{\sigma_J^2 + \sigma_b^2}$, μ m
$erf\ (x)$ = Error function, $2/\pi \int_0^x \exp(-y^2)dy$
R = Regression parameter for ANN training

Non-dimensional Parameters

$\bar{h}, \bar{h}_L, \bar{h}_T = (h, h_L, h_T)/c$
$\bar{C}_{s2} = \frac{1}{12} \times \left(\frac{\pi r_c^4}{8c^3 l_c} \right)$, Restrictor Design Parameter
$\bar{h}_{\min}$ = Minimum oil film thickness, $h_{\min}/c$
$\bar{M}_j$ = Journal mass, $M_J \left(c^5 p_s / \mu^2 R_J^6 \right)$
$\bar{M}_{CJ}$ = Critical journal mass, $M_{cj} \left(c^5 p_s / \mu^2 R_J^6 \right)$
$\bar{T}_{FJ}$ = Frictional torque on journal surface
$(p, \bar{p}_c) = (p, \bar{p}_c)/p_s$
$(\bar{V}_{rj}, \bar{V}_{rb})$ = Variance ratio of journal and bearing, $\left((\sigma_j, \sigma_b)/\sigma\right)^2$
$\bar{w}$ = $w(\mu R_J / c^2 p_s)(R_J/c)$
$\bar{z}$ = (z/h_L), in a rough bearing
$(\bar{X}_J, \bar{Z}_J)$ = Journal centre coordinates, $(X_J, Z_J)/c$
α = Circumferential coordinate, (x/R_J)
β = Axial coordinate, (y/R_J)
γ = Surface pattern parameter, $\frac{\lambda_{0.5x}}{\lambda_{0.5y}}$
Λ = Surface roughness parameter, (c/σ)
Ω = Speed parameter, $\omega_J \left(\mu R_J^2 / c^2 p_s \right)$
$\bar{\tau}_{xz_j}$ = Shear stress, $\tau_{xz_j} \left(R_J / c p_s \right)$

III. METHODOLOGY

Methodology is framed in the present work includes the development of hole-entry hybrid journal bearing simulation model to compute performance parameters of hybrid journal bearings and development of integrated Artificial Neural Networks (ANNs) and multi objective Genetic Algorithms (MOGA) for the optimization of bearing. Fig 1 illustrated the flow chart of optimization process of hole-entry hybrid journal bearing shown in Fig. 2. The development of overall optimization process includes the following main steps:

IV. SELECTION OF DESIGN VARIABLES AND OBJECTIVE FUNCTIONS

This step involves the selection of geometric and operating design variables of hole-entry hybrid journal bearing. Design variables such as supply pressure, restrictor design parameter and dynamic viscosity as well as roughness characteristics such as variance ratio and roughness pattern parameters are selected to optimize. The combination of such variables generates large number of data for the ANN input design variables.

ISSN: 2321-9653; IC Value: 45.98; SJ Impact Factor: 7.177
Volume 7 Issue VII, July 2019- Available at www.ijraset.com

The minimum fluid film thickness ($\bar{h}_{\min}$), frictional torque on journal surface ($\bar{T}_{Fj}$) and critical journal mass ($\bar{M}_{cj}$) of capillary compensated hole-entry hybrid journal bearing are selected as objective functions.

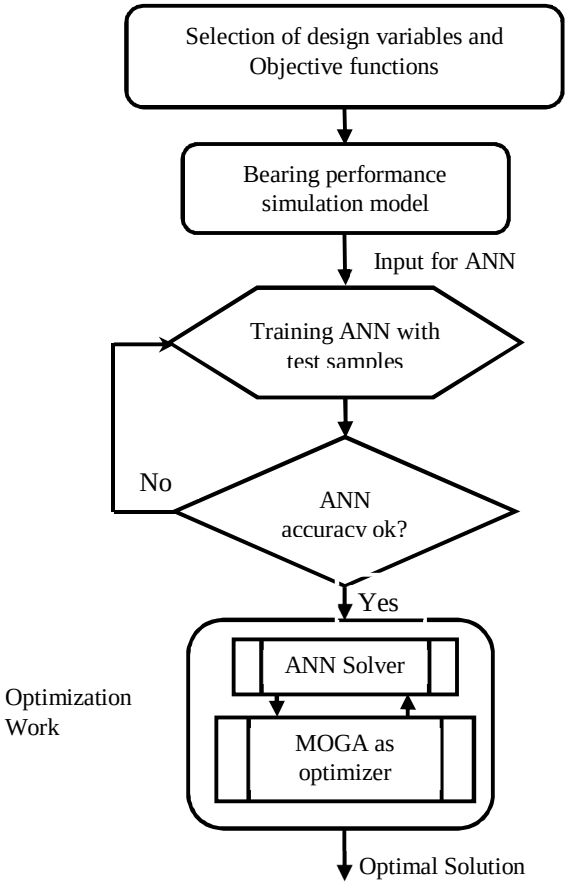

Fig 1: Overall flowchart of optimization process

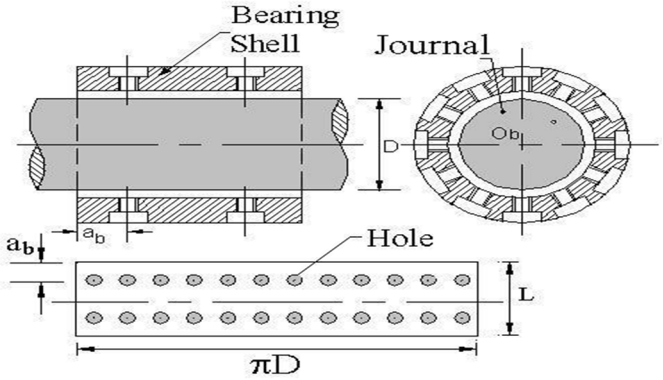

Fig 2: Hole-entry hybrid journal bearing

V. BEARING PERFORMANCE SIMULATION MODEL

Training of ANN requires target values for the selected input design variables selected. These target values are the output results of selected objective functions obtained from the computer code written for the mathematical models. These mathematical models include the expressions for fluid-film thickness, Reynolds equation, restrictor flow equation, etc. for the computation of performance of hole-entry hybrid journal bearing. These expressions are numerically solved using finite element method to obtain the fluid pressure and there by performance of bearing. The following expressions are used in this bearing performance simulation model.

ISSN: 2321-9653; IC Value: 45.98; SJ Impact Factor: 7.177
Volume 7 Issue VII, July 2019- Available at www.ijraset.com

A. Average Reynolds Equation

The average Reynolds equation governing the laminar flow of an incompressible, Newtonian lubricant in the clearance space between rough surface of journal and bearing in non-dimensional form is written as [10]

$$\frac{\partial}{\partial\alpha}\left(\phi_x\frac{\bar{h}^3}{12}\frac{\partial\bar{p}}{\partial\alpha}\right)+\frac{\partial}{\partial\beta}\left(\phi_y\frac{\bar{h}^3}{12}\frac{\partial\bar{p}}{\partial\beta}\right)=\frac{\Omega}{2}\frac{\partial\bar{h}_T}{\partial\alpha}+\frac{\Omega}{2\Lambda}\frac{\partial\phi_s}{\partial\alpha}+\frac{\partial\bar{h}_T}{\partial\tau} \quad (1)$$

where ϕ_x,ϕ_y are flow factors used to compare the average pressure flows (in axial and circumferential directions) in a rough journal bearing to that of smooth bearing and ϕ_s is the shear flow factor which represent the additional flow transport of lubricant in circumferential direction due to sliding of rough journal. These flow factors can be obtained from Patir and Cheng [11, 12]

B. Average Fluid-film Thickness

For the fully lubricated ($\Lambda\bar{h}>3$) and partially lubricated ($\Lambda\bar{h}\le 3$) regions, the average fluid-film thickness, $\bar{h}_T$ appeared in Eq. (1) is expressed in non-dimensional form as [10]

$$\bar{h}_T=\begin{cases}\bar{h} & \text{for } \Lambda\bar{h}>3\\ \dfrac{\bar{h}}{2}\left(1+erf\left(\dfrac{\Lambda\bar{h}}{\sqrt{2}}\right)\right)+\dfrac{1}{\Lambda\sqrt{2\pi}}e^{-(\Lambda\bar{h})^2/2} & \text{for } \Lambda\bar{h}\le 3\end{cases} \quad (2)$$

where $\bar{h}$ is the nominal fluid-film thickness expressed as [10]

$$\bar{h}=1-\bar{X}_J\cos\alpha-\bar{Z}_J\sin\alpha \quad (3)$$

C. Boundary Conditions

The following boundary conditions are used for the solution of Reynolds Eq. (1):

1) Nodes situated on the external boundary of the bearing have zero pressure, $\bar{p}\big|_{\beta=\pm1}=0$

2) At the supply hole, $\bar{p}=\bar{p}_s=1$

3) At the trailing edge of the positive region, $\bar{p}=\dfrac{\partial\bar{p}}{\partial\alpha}=0$

D. Restrictor flow Equation

The flow equation for capillary restrictor is expressed in non-dimensional form as [10]

$$\bar{Q}_R=\bar{C}_{s2}\left(1-\bar{p}_c\right) \quad (4)$$

The above equations are solved using finite element method to obtain pressure field in the clearance space of hole-entry hybrid journal bearing. Using this pressure field, the journal centre equilibrium position for the specified vertical load is established as explained by Nagaraju et. al [10]. Once the journal centre equilibrium position is established, the results for the objective functions such as minimum fluid-film thickness, frictional torque and critical journal mass of the bearing are computed using the following expressions.

1) Minimum fluid-film Thickness: The nominal fluid-film thickness at each node of discretized flow field is computed using Eq. (3). Then the minimum fluid-film thickness is selected as

$$\bar{h}_{\min}=\text{minimum of }\left\langle\bar{h}\right\rangle_n,\ n=1,2,.....,n_l \quad (5)$$

where, n_l is the number of nodes in the discretized flow field domain.

2) Frictional Torque: The frictional torque on the journal surfaces is obtained from

$$\bar{T}_{Fj}=\int_{-\lambda}^{\lambda}\int_{0}^{2\pi}\bar{\tau}_{xz_j}\,d\alpha\,d\beta \quad (6)$$

where $\bar{\tau}_{xz_j}$ is the shear stress on journal surface and is expressed as [12]

ISSN: 2321-9653; IC Value: 45.98; SJ Impact Factor: 7.177
Volume 7 Issue VII, July 2019- Available at www.ijraset.com

$$\bar{\tau}_{zx_j} = \frac{\Omega}{\bar{h}}(\phi_f + \phi_{fs}) + \phi_{fp}\frac{\bar{h}}{2}\frac{\partial \bar{p}}{\partial \alpha} \quad (7)$$

where ϕ_f, ϕ_{fs} and ϕ_{fp} are shear stress factors and are obtained from Patir and Cheng [12].

E. Critical Journal Mass

Critical journal mass, in the present work is obtained by using Routh's stability criteria.

VI. ARTIFICIAL NEURAL NETWORK IMPLEMENTATION

In this work, ANN implementation, training and testing are done using the 'neural network toolbox' of MATLAB. Three different ANNs are built rather than using one large ANN for the generation output variables for three objective functions of the problem. This strategy allowed for better adjustment of the ANN for each specific problem, including the optimization of the architecture for each output. The list of inputs (i.e. design variables) and targets are shown in Tables 1 and 2, respectively. Totally 567 samples of data are generated, among which 550 of them are used for ANN training and 17 samples are kept for ANN testing. For each ANN, the input layer uses 6 nodes and the output layer uses 1 node. The training and testing parts of the developed ANN are done using the output results obtained from bearing performance simulation model for the set of input design variables. Output results for the objective functions listed in Table 2 are computed for the following fixed values of operating and geometric parameters of the bearing:

Bearing speed = 3000 rpm, maximum load on bearing = 15000 N, aspect ratio, $\lambda = 1$, radial clearance = 0.05mm, journal radius = 50mm and Surface roughness parameter, $\Lambda = 25$.

The Mean Squared Error (MSE) shown in Eq. (8) is selected as the performance function inside the neural network.

$$MSE = \frac{1}{N}\sum_{i=1}^{N}\left(e^i\right)^2 = \frac{1}{N}\sum_{i=1}^{N}\left(X_{real}(i) - X_{predicted}(i)\right)^2 \quad (8)$$

Since the MSE is calculated for each iteration, it can't be used as the overall neural network performance parameter. A regression parameter R is used to assess the overall network performance.

$$R = Target / Output \quad (9)$$

where, targets are the objective values and the outputs are the actual values produced by ANN. There should be close agreement in R so that the ANN can be used to generate missing data in the bearing simulation during the optimization process. After the confirmation of ANN prediction quality, it is used for multi objective optimization problem in GA.

Table 1: List of inputs for ANN

Sl. No.	Inputs	Range of variation	Interval	Units
1	Variance ratio, $\bar{V}_{rj}$	0 – 1	0.5	-
2	Supply Pressure, p_s	8 – 12	2	N/m^2
3	Restrictor Design Parameter, $\bar{C}_{s2}$	0.05 - 0.13	0.04	-
4	Dynamic viscosity, μ	0.026 – 0.046	0.01	Pas
5	Surface pattern parameter, γ	1/3, 1/6, 1/9, 1, 3, 6, 9	-	-

Table 2: List of targets for ANN

Sl. No.	Outputs	Definition	Units
1	$\bar{h}_{min}$	Minimum oil film thickness	-
2	$\bar{T}_{FJ}$	Frictional torque on journal surface	-
3	$\bar{M}_{CJ}$	Critical journal mass	-

VII. ANN TRAINING QUALITY

Figures 3 to 5 shows the performance, training state and regression plots of ANN developed for the minimum fluid-film thickness ($\overline{h}_{\min}$) as target function. It is clear from Fig. 3 that the validation, training and testing performance curves trend are almost same. But in the end, the testing curve deviating from training and validation curves. The MSE of the network when stopped was observed to be of 7.66e-7 within 2 seconds which is a comparatively good value. The best validation performance value is observed to be 6.189e-007 at epoch 54 just 6 epochs before the training stopped and it is far less than the set value of 0.001. As seen from Fig. 4, the mu (μ) value decreases for each step indicating shifting towards more efficient Newton's method from gradient descent technique. Fig. 5 shows a maximum regression (R) value of 99.958 % which is a very good value for the amount of data used to validate.

As seen from Figs. 6 to 8, ANN training for second network developed for critical journal mass ($\overline{M}_{CJ}$) as the target function achieved a MSE of only 2.74e-05, but took 303 epochs and 6 seconds until the training stopped due to validation fail at 297 epoch. It achieved a average regression value of 99.993%.

Figures 9 to 11 shows the performance, training state and regression plots of ANN for target function frictional torque ($\overline{T}_{Fj}$). Training took place for 2 seconds and 29 epochs by achieving the MSE value of 0.0130 and the average regression value of 99.962% is achieved.

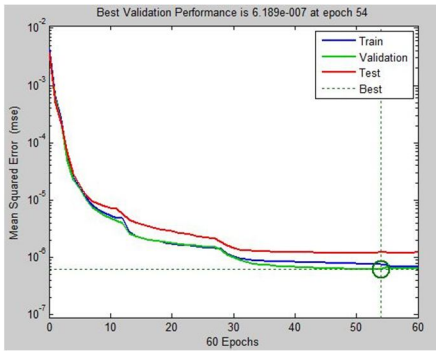

Fig 3: ANN performance plot for $\overline{h}_{\min}$

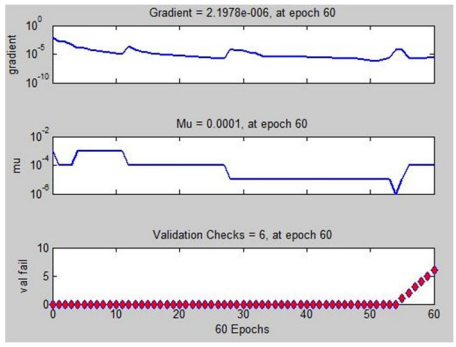

Fig 4: ANN training state for $\overline{h}_{\min}$

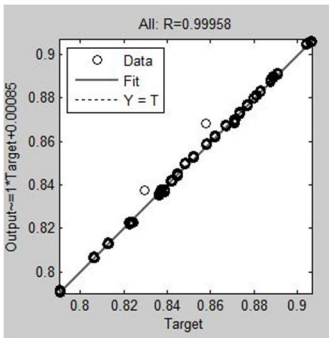

Fig 5: ANN regression plot for $\overline{h}_{\min}$

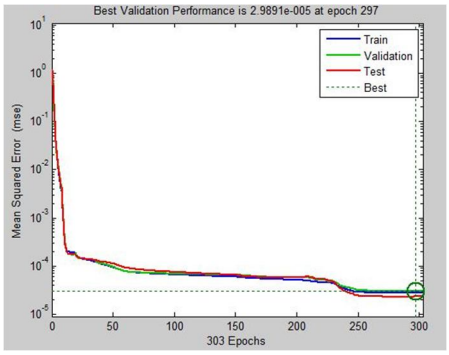

Fig 6: ANN performance plot for $\overline{M}_{CJ}$

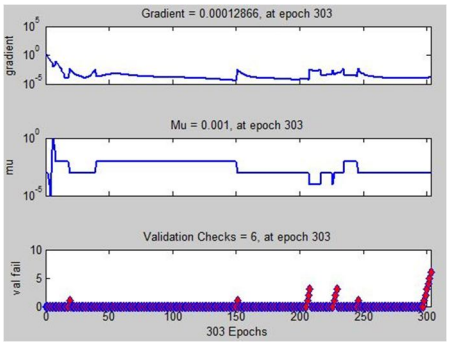

Fig 7: ANN training state for $\overline{M}_{CJ}$

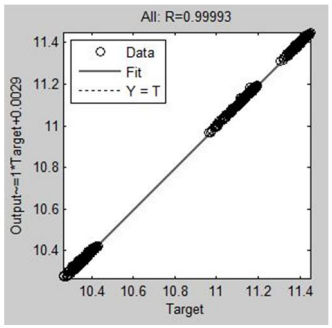

Fig 8: ANN regression plot for $\overline{M}_{CJ}$

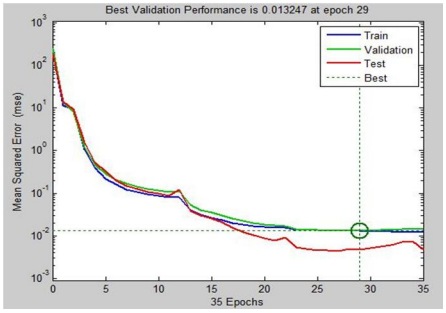

Fig 9: ANN performance plot for $\overline{T}_{FJ}$

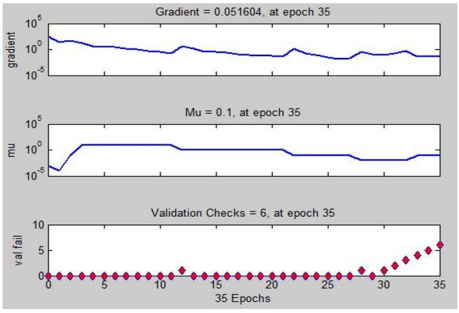

Fig 10: ANN training state for $\overline{T}_{FJ}$

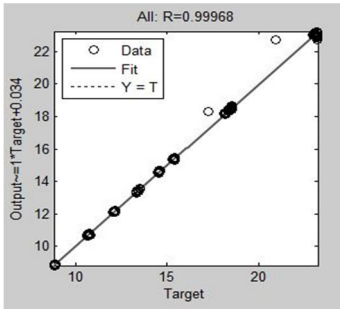

Fig 11: ANN regression plot for $\overline{T}_{FJ}$

ISSN: 2321-9653; IC Value: 45.98; SJ Impact Factor: 7.177
Volume 7 Issue VII, July 2019- Available at www.ijraset.com

VIII. GENETIC ALGORITHM IMPLEMENTATION

The optimization of hole-entry journal bearing is a nonlinear multi-objective optimization problem with moderate complexity–three objective functions, six parameters and with constraints. Therefore, a Multi-Objective Genetic Algorithm (MOGA) is developed using the 'global optimization toolbox' in MATLAB. MOGA solver attempts to create a set of Pareto optima for a multi-objective minimization. MOGA uses the genetic algorithm for finding local Pareto optima.

After confirming the accuracy of ANN, it is further used as a part of the optimization tool with genetic algorithm. Primary requirement for solving the optimization problem using GA is the objective function. Prediction model of ANN can be used as an objective function. MATLAB code is written in such a way that ANN prediction tool is activated simultaneously as GA starts the optimization process.

To obtain 2D Pareto front plot, the 3 objective functions are arranged in 3 combinations comprising 2 objective functions in each combination so as to obtain the best design options for these combinations.

IX. OPTIMIZATION RESULTS

The maximization of minimum oil film thickness (MOFT) and critical journal mass as well as the minimization of frictional torque has been separately carried out for the capillary compensated hole-entry journal bearing having transverse roughness pattern ($\gamma = 1/6$). The optimization results of variance ratio ($\bar{V}_{rj}$), supply pressure (p_s), restrictor design parameter ($\bar{C}_{s2}$) and dynamic viscosity (μ) for the maximization of MOFT ($\bar{h}_{\min}$) and critical journal mass ($\bar{M}_{cj}$) and minimization of friction torque ($\bar{T}_{Fj}$) are presented in the form of Pareto front in Figures 12 to 14. Since MOGA always performs the minimization of any objective functions, the maximization of required objective function can be obtained by assigning negative value so that minimization of negative objective function is same as its maximization. Hence maximization of objective functions can be obtained from these entire Pareto front plots by neglecting its negative values.

A. Optimization Results for Maximization of $\bar{h}_{\min}$ and Minimization of $\bar{T}_{FJ}$

Figure 12 shows the Pareto front for the combination of objective functions $\bar{h}_{\min}$ and $\bar{T}_{FJ}$ of the bearing. Pareto optimal front provides 25 design options, among which the best ones are to be selected from the plot. From Fig. 12, it can be seen that the frictional torque $\bar{T}_{FJ}$ drastically decreases for the design option 1 (point A) to 24 (point B) with marginal decrease in the value of MOFT ($\bar{h}_{\min}$). From the design options 24 (point B) and 25 (point C), the decrease in the value of $\bar{T}_{FJ}$ is marginal and reduction in the value of $\bar{h}_{\min}$ is significant. Therefore, the design option 24 (point B) can be considered as a best option. The optimized design variables for this combination of objective functions of journal bearing is tabulated in Table 3. If the designer priority is to have minimum frictional torque, then the design option 25 (point C) which provides minimum $\bar{T}_{FJ}$ keeping $\bar{h}_{\min}$ value between 0.85 and 0.86 can be selected.

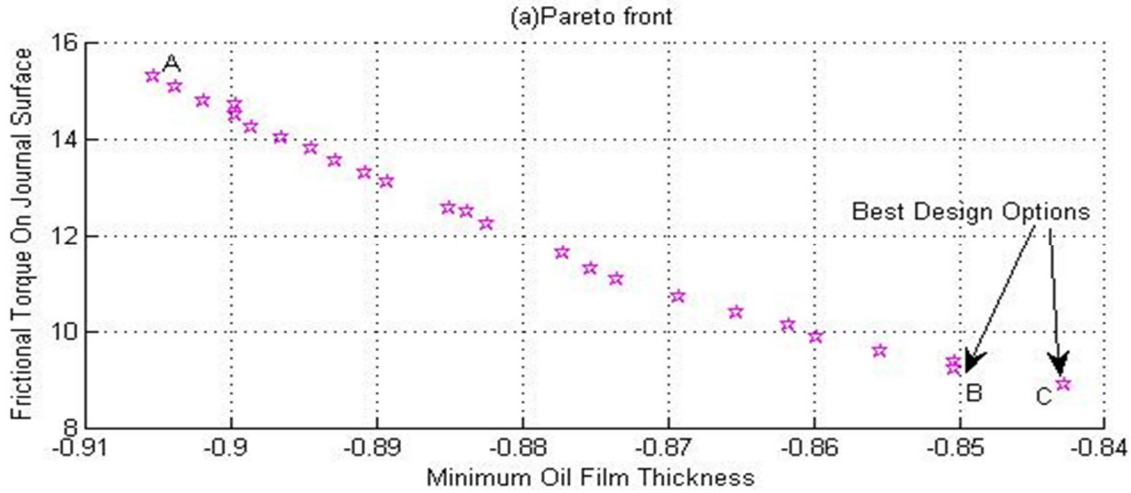

Fig 12: MOGA results for maximization of $\bar{h}_{\min}$ and minimization of $\bar{T}_{Fj}$ of journal bearing

ISSN: 2321-9653; IC Value: 45.98; SJ Impact Factor: 7.177
Volume 7 Issue VII, July 2019- Available at www.ijraset.com

B. Optimization results for Maximization of $\bar{h}_{min}$ and Maximization of $\overline{M}_{CJ}$

For the maximization of $\bar{h}_{min}$ and $\overline{M}_{CJ}$, the pareto front provides 26 design options as shown in Fig. 13. It can be seen that as the design option changes from option 1 (point A) to option 26 (point B), the critical mass ($\overline{M}_{CJ}$) increases significantly while the minimum oil film thickness, $\bar{h}_{min}$ decreases very marginally. The critical journal mass increased by 12.72% while MOFT decreased by only 2.71% as design option changes from 1 to 26. It can be seen from Fig. 13 that the design options which provide the maximum enhancement to $\bar{h}_{min}$ are fail to provide enhanced value of $\overline{M}_{CJ}$. Thus, as a compromise the last 26th design option (point B) which provides maximum possible enhancement to $\overline{M}_{CJ}$ with minimum but acceptable value of $\bar{h}_{min}$ can be selected as best design option. The optimized design variables for this combination of objective functions of journal bearing are tabulated in Table 3.

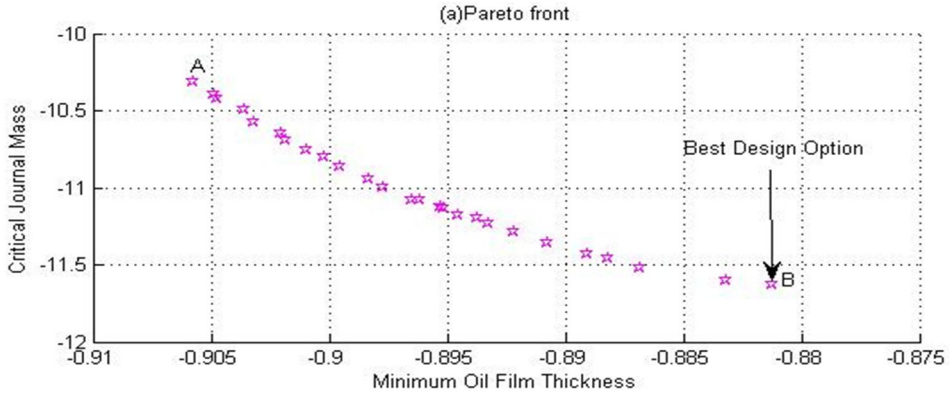

Fig 13: MOGA results for maximization of $\bar{h}_{min}$ and minimization of $\overline{M}_{CJ}$ of journal bearing

C. Optimization results for maximization of $\overline{M}_{CJ}$ and minimization of $\overline{T}_{FJ}$:

Figure 14 shows the Pareto front for the combination of objective functions $\overline{M}_{CJ}$ and $\overline{T}_{FJ}$. This pareto front provides totally 25 design options for this combination. The value of both $\overline{T}_{FJ}$ and $\overline{M}_{CJ}$ decreases as the design options changes from option 1 to option 25. Frictional torque $\overline{T}_{FJ}$ reduces significantly for the options 1 (point A) to 22 (point B) while critical journal mass $\overline{M}_{CJ}$ reduces marginally. The design options 22 to 25 doesn't give any benefit as there is a considerable reduction in the value of $\overline{M}_{CJ}$ with negligible reduction in the value of $\overline{T}_{FJ}$. Hence, it is suitable to select the design option 22 (point B) as the optimum design with maximum $\overline{M}_{CJ}$ and minimum $\overline{T}_{FJ}$. The optimized design variables for this combination of objective functions of journal bearing are tabulated in Table 3.

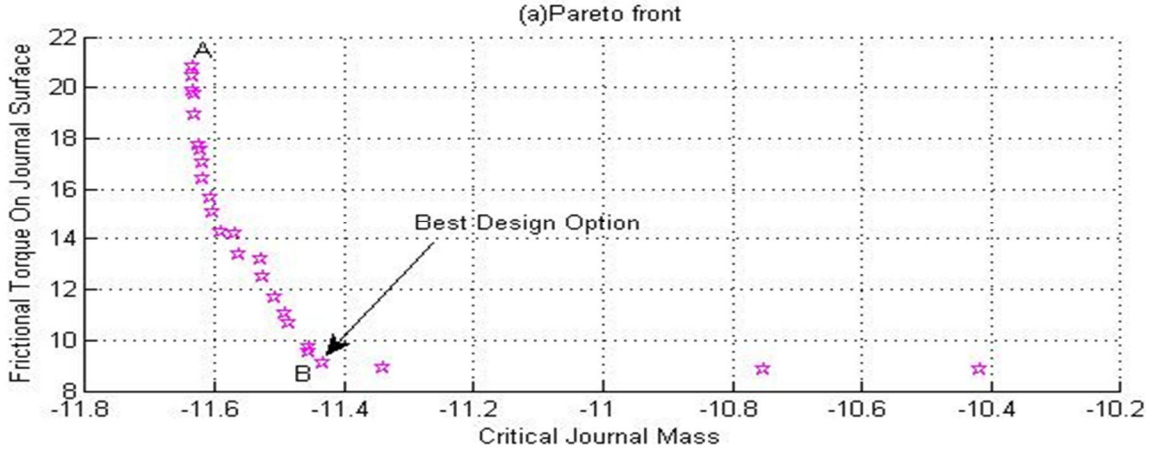

Fig 14: MOGA results for maximization of $\bar{h}_{min}$ and minimization of $\overline{M}_{CJ}$ of journal bearing

Table 3: Pareto optimal design options for combination of objective functions.

Combinations	Design Options	$\bar{h}_{\min}$	$\bar{T}_{FJ}$	$\bar{M}_{CJ}$	$\bar{V}_{rj}$	p_s (N/m^2)	$\bar{C}_{s2}$	μ (Pas)
$\bar{h}_{\min}$ v/s $\bar{T}_{FJ}$	24	0.85032	9.202511	-	0.527891	11.98356	0.055436	0.027309
	25	0.84282	8.874032	-	0.546408	11.983	0.066899	0.026035
$\bar{h}_{\min}$ v/s $\bar{M}_{CJ}$	26	0.88127	-	11.6278	0.988054	9.939482	0.103837	0.045628
$\bar{M}_{CJ}$ v/s $\bar{T}_{FJ}$	22	-	9.115527	11.4341	0.860832	11.79958	0.095465	0.026374

X. CONCLUSIONS

A. Multi-Objective Genetic Algorithm (MOGA) has been developed and customized to use the Artificial Neural Network simulation results of objective functions for the optimization process of capillary compensated hole-entry hybrid journal bearing.

B. Achievement of regression value above 99% and close agreement between expected and predicted value of all the three output functions shows the suitability of ANN in Multi-objective Genetic Algorithm optimization problem.

C. Using MOGA technique, the maximization of minimum oil film thickness and critical journal mass and minimization of frictional torque have been separately carried out for the bearings having transverse type roughness patterns.

D. The optimization process was carried out for the optimization of design variables: variance ratio, supply pressure, restrictor design parameter and dynamic viscosity. Further Pareto optimal concept was utilized to predict the best design options for the maximization and/or minimization of two selected objective functions together.

REFERENCES

[1] Hashimoto.H., (1997), "Optimum design of high speed short journal bearings by Mathematical programming," STLE Tribol. Trans., vol. 40, no. 2, pp. 283-293.

[2] Hashimoto.H., and Matsumoto.K., (2000), "Improvement of Operating Characteristics of High-Speed Hydrodynamic Journal Bearings by Optimum Design: Part I – Formulation of Methodology and Its Application to Elliptical Bearing Design," ASME. Jr. of Tribo., vol.123, pp. 305-312.

[3] Wang N., Li Ho C. and ChaK. C., (2000), Engineering optimum design of fluid-film lubricated bearings, STLE Tribo. Trans., vol. 43, no. 3, pp. 377-386.

[4] Hirani.H., and Suh.N.P., (2005), "Journal bearing design using multi-objective genetic algorithm and axiomatic design approaches," Tribol. Int., vol. 38, pp.481-491.

[5] Boedo S., and Eshkabilov S. L., (2002), Optimal shape design of finite width journal bearings using genetic algorithm," Proc. of ASME/STLE Joint Int. Tribo. Conf., Cancun, Maxico.

[6] Ghorbanian.J., Ahmadi.M., and Soltani.R., (2011), "Design predictive tool and optimization of journal bearing using neural network model and multi-objective genetic algorithm," Scientia Iranica, vol. 18, no. 5, pp.1095-1105.

[7] Kirankumar B. M. and Prajapati J. M., (2012), A brief review on optimum design of a journal bearings for I.C. engine," Int. Jr. of Engg. Resea. and Techol., vol. 1, no. 4, pp. 1-9.

[8] Roy L., and Kakoty S. K., (2013), Optimum groove location of hydrodynamic journal bearing using genetic algorithm, Advances in Tribo. Article ID 580367, pp. 1-13.

[9] Cook D. F., Ragsdale C. T., and Major R. L., (2000), Combining a neural network with a genetic algorithm for process parameter optimization, Engg. Appli. of Artificial Intelligence, vol. 13, pp. 391-396.

[10] Nagaraju.T., Sharma.S.C., and Jain.S.C., (2002), "Influence of surface roughness effects on the performance of non-recessed hybrid journal bearings," Tribology International. vol. 35, no. 7, pp.467-487.

[11] Patir N. and Cheng H. S., (1978), "An Average Flow Model for Determining Effect of Three-Dimensional Roughness on Partial Hydrodynamic Lubrication", Trans. ASME Jr. of Lub. Tech., vol. 100, pp. 12-17, 1978.

[12] Patir N. and Cheng H. S., (1979), "Application of Average Flow Model to Lubrication between Rough Sliding Surfaces", Trans. ASME Jr. of Lub. Tech., vol. 101, pp. 220-230.

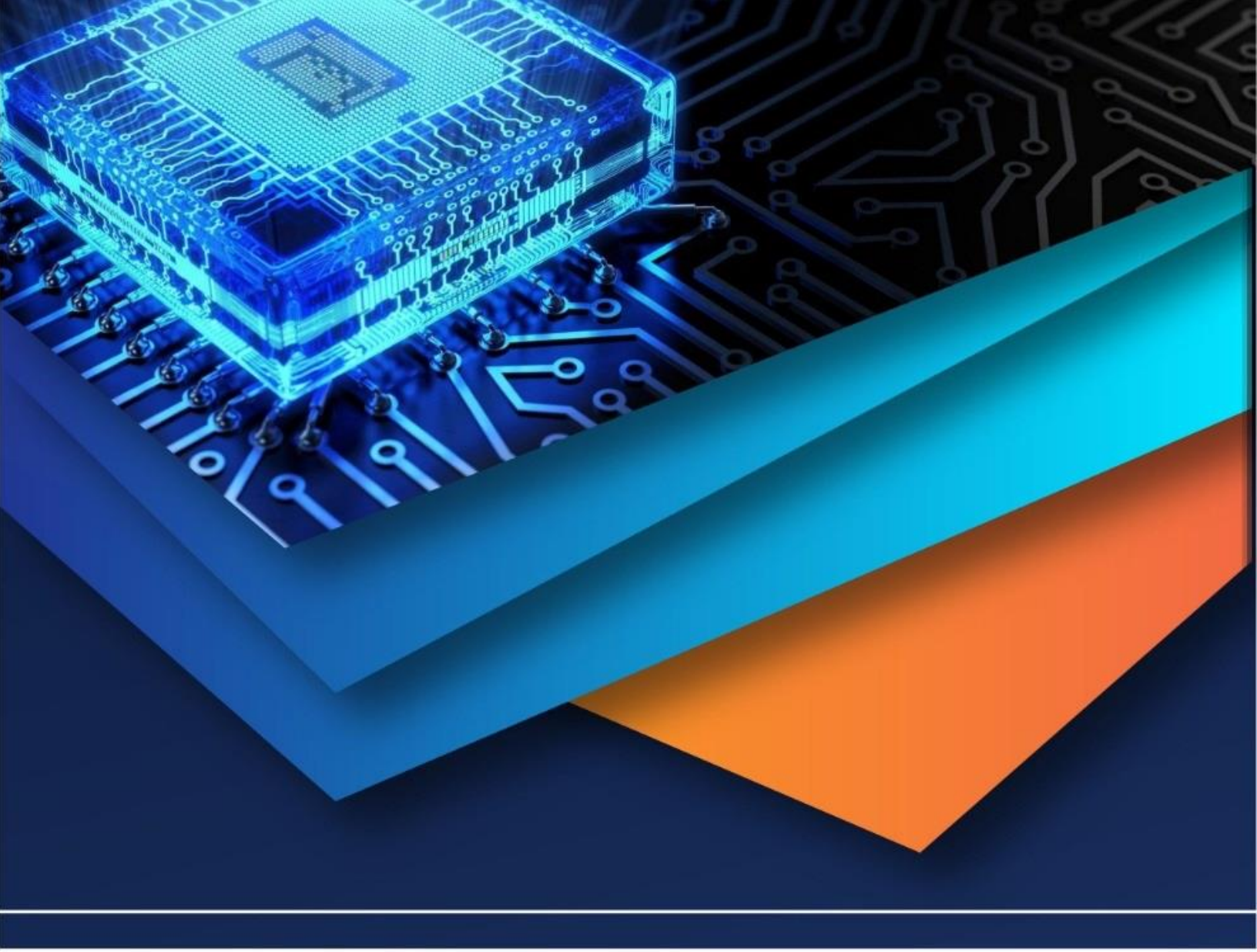

10.22214/IJRASET

45.98

IMPACT FACTOR: 7.129

IMPACT FACTOR: 7.429

INTERNATIONAL JOURNAL FOR RESEARCH

IN APPLIED SCIENCE & ENGINEERING TECHNOLOGY